Original Research Article

NANOBIOMEDICINE

Nanobiomedicine
Volume 5: 1–9
© The Author(s) 2018
Article reuse guidelines:
sagepub.com/journals-permissions
DOI: 10.1177/1849543518803538
journals.sagepub.com/home/nab
SAGE

Engineering the hard–soft tissue interface with random-to-aligned nanofiber scaffolds

John Nowlin[1], Mehzubh A Bismi[1], Baptiste Delpech[2], Patrick Dumas[3], Yingge Zhou[4], and George Z Tan[4]

Abstract

Tendon injuries can be difficult to heal and have high rates of relapse due to stress concentrations caused by scar formation and the sutures used in surgical repair. Regeneration of the tendon/ligament-to-bone interface is critical to provide functional graft integration after injury. The objective of this study is to recreate the tendon-to-bone interface using a gradient scaffold which is fabricated by a one-station electrospinning process. Two cell phenotypes were grown on a poly-ϵ-caprolactone nanofiber scaffold which possesses a gradual transition from random to aligned nanofiber patterns. We assessed the effects of the polymer concentration, tip-to-collector distance, and electrospinning time on the microfiber diameter and density. Osteosarcoma and fibroblast cells were seeded on the random and aligned sections of scaffolds, respectively. A random-to-aligned cocultured tissue interface which mimicked the native transition in composition of enthesis was created after 96 h culturing. The results showed that the microstructure gradient influenced the cell morphology, tissue topology, and promoted enthesis formation. This study demonstrates a heterogeneous nanofiber scaffold strategy for interfacial tissue regeneration. It provides a potential solution for mimicking transitional interface between distinct tissues, and can be further developed as a heterogeneous cellular composition platform to facilitate the formation of multi-tissue complex systems.

Keywords

Electrospinning, tissue engineering, heterogeneous nanofiber scaffold, enthesis, tendon

Date received: 6 June 2018; accepted: 29 August 2018

Introduction

Tendons are fibrous connective tissues in the human body that connect muscle to bone. They allow for joint movement and are primarily made up of collagen type I fiber bundles along with a small amount of other types of cells and materials.[1] Healthy tendon fibers are oriented in a parallel manner and are capable of transferring high tensile loads between tendon and bone.[2] The interface in which the tendon connects to the bone is composed of a specialized transitional tissue with varying structures and compositions.[1] More importantly, collagen fibers at the bone section of the interface are significantly less oriented when compared with fibers in the tendon.[3]

Tendinopathy, also known as disease or damage to the tendon, consists of various types of injury which can be

[1] Department of Mechanical Engineering, Texas Tech University, Lubbock, Texas, USA
[2] Department of Chemical Engineering, Texas Tech University, Lubbock, Texas, USA
[3] Department of Biomedical Engineering, Texas Tech University, Lubbock, Texas, USA
[4] Department of Industrial, Manufacturing & Systems Engineering, Texas Tech University, Lubbock, Texas, USA

Corresponding author:
George Z Tan, Department of Industrial, Manufacturing & Systems Engineering, Texas Tech University, Box 43061, Lubbock, TX 79409-3061, USA.
Email: george.z.tan@ttu.edu

Creative Commons Non Commercial CC BY-NC: This article is distributed under the terms of the Creative Commons Attribution-NonCommercial 4.0 License (http://www.creativecommons.org/licenses/by-nc/4.0/) which permits non-commercial use, reproduction and distribution of the work without further permission provided the original work is attributed as specified on the SAGE and Open Access pages (https://us.sagepub.com/en-us/nam/open-access-at-sage).

caused by many different factors, both intrinsic and extrinsic. Physical activity leading to excessive loading of tendons is the primary cause for degeneration.[4] Also, intrinsic factors such as alignment and biomechanical faults account for two-thirds of athletes with Achilles tendon disorders.[4] Injury of the tendon can be acute or chronic, and generally results in inflammation and/or degeneration, which can lead to tendon rupture. Current methods to reattach tendon to bone use sutures that result in increased stress concentrations, leading to high failure rates for surgical repairs.[5] Additionally, while a healthy interface is made up of a gradient of different cell types which reduce stress concentrations between the bone and tendon, healing of this interface after damage can result in scar tissue formation, rather than a proper regeneration of the original tissue.[6] Because of this complexity, there is a need to replace the tendon-to-bone interface.

Tissue engineering has emerged as a promising therapeutic alternative for tissue injuries and lesions.[7] To regenerate the native tissues, cells are harvested from their natural environment and grown in an artificial scaffold under controlled conditions. The ideal scaffold should provide not only a physical support for cell to attach and proliferate, but also microstructure cues to mimic the native extracellular matrix (ECM) to guide the cell growth and organization. This scaffold orientation not only affects the direction of cellular growth but also results in different gene expression between different scaffold microstructures.[8] It remains a challenge to establish an anisotropic microenvironment for a complex tissue structure with multiple cell types. To address this problem, this study focuses on the bone-to-tendon tissue regeneration using electrospun random-to-aligned nanofiber scaffold.[1]

Electrospinning is a process that creates polymeric fibers with diameters ranging from 1 μm to 100 nm. A positive voltage is applied to a liquid solution which is then pushed through a needle. A target attached to ground or a negative voltage then attracts the solution. This target determines the orientation of the resulting fibers, with stationary flat targets gathering randomly oriented fibers and targets rotating on an axis parallel to the electrospinning creating aligned fibers.[9] Two stationary targets with a gap between them result in randomly oriented fibers on the targets and aligned fibers bridging between them.[9] This process can be used for a wide variety of tissue engineering applications, such as nanocomposite/hybrid approaches for mimicking bone tissue.[10]

There have also been numerous different techniques attempting to improve various stages of the electrospinning process, including water-friendly core designs, nanocapsule/nanofibrous sheathes,[10] and melt-electrospinning techniques.[11] Electrospinning into a water bath with a solution of water-soluble and non-water-soluble polymers has shown to increase fiber porosity, which promotes cell attachment and growth.[12] Coaxial electrospinning can be utilized to fine-tune the mechanical properties of the scaffold without changing the overall fiber diameter or surface characteristics by adjusting the core fiber material and diameter.[13] Co-electrospinning, or electrospinning with two materials simultaneously, has been successfully shown to create two distinct uniform regions with a gradient region in between which allows for the selection of materials with similar properties to the natural muscle–tendon interface.[14] A similar technique was used with one material doped with nano-hydroxyapatite then submerged in simulated body fluid to selectively grow hydroxyapatite in a gradient.[15]

To create the random-to-aligned nanofiber scaffold, we adopted a parallel-collector configuration in which two grounded metal bars were placed in parallel under the spinneret. The fibers collected on the target form two distinct regions, a randomized region on the metal bars, and an aligned region that spans between the parallel bars. Fibroblasts and osteosarcoma cells were seeded onto the aligned region and the random region, respectively. These two types of cells were cocultured in a single scaffold to mimic the cellular organization in the tendon-to-bone interface. We demonstrated that the gradients in scaffold microtopology will facilitate cell organization and promote the formation of the tendon-to-bone interface in a coculturing environment *in vitro.*

Materials and methods

Electrospinning

Electrospinning was performed with 15% and 20% w/v of polycaprolactone (PCL) in acetone and dimethylformamide (DMF) solution with a ratio 1:1, which is often used for medical applications.[16] The solution was put in a syringe attached to a controlled rate pump, and a positive voltage was attached to a needle at the end of the syringe. The pump rate and voltage were adjusted to ensure consistent electrospinning. Parallel aluminum bars were placed 3.5 cm apart and connected to a negative voltage source, to use as the target. This setup can be seen in Figure 1(a). Thin glass squares with side length of 2 cm were placed partially on the bar with the rest in the gap between the bars to facilitate sample preparation and prevent the material from folding on itself. The distance between the tip of the needle and top of the target was set at 15 cm and 20.5 cm, and the placement of the target was adjusted to keep the fibers centered on the target. Once everything was set up and spinning without issue, the electrospinning process was run for 5 and 10 min per sample. The electrospun material was then cut along the edge of the glass square. These samples were then used for imaging or for cellular growth. Some additional samples were spun in the same manner to start, but halfway through a cover was placed over the random section to reduce its fiber density. The fibers on the cover were then cut along the edge of the cover prior to its removal (Figure

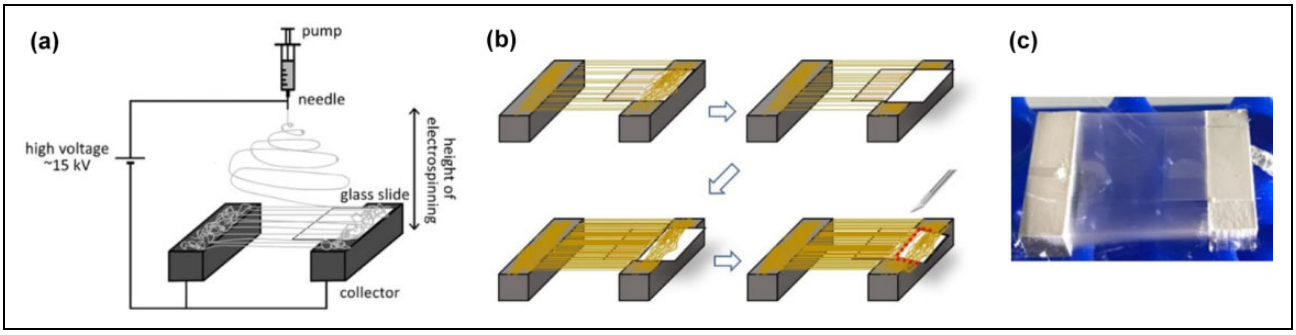

Figure 1. Electrospinning configuration: (a) represents the general configuration of our electrospinning technique; (b) illustration of collecting the aligned-to-random nanofiber scaffold; and (c) shows the result of the electrospinning for the second sample (15% PCL, 10-min duration, 15 cm height). PCL: polycaprolactone.

1(b)). This was done to achieve a more uniform fiber thickness between the random section and the aligned, because a large disparity in thickness would occur between these two sections if the electrospinning continued.

Scaffold characterization

The electrospun samples were gold sputtered for 45 s using the sputtering equipment. One of the samples was then carefully placed onto a carbon-taped sample holder without air getting trapped between the sample and the carbon tape. Using both light optical and electron optical modes, the samples were observed under Phenom ProX scanning electron microscope (SEM, Nanoscience Instrument, Phoenix, AZ). ProSuite, the built-in equipment software was used to capture images of random, transition, and aligned fiber regions of the sample. Magnification of 2000× was used for determining the alignment of the fiber and 10,000× was used to determine the diameter of the fiber. The saved images were then transferred to a computer to quantify the diameter distribution, fiber orientation, as well as the porosity using ImageJ (Version 1.8.0).

Cell culture

Electrospun samples were sterilized by ultraviolet exposure for 30 min. Two different fluorescent cell trackers (CellTracker™, ThermoFisher Scientific, Wartham, MA), CM-DIL ($C_{68}H_{105}Cl_2N_3O$) and CMAC ($C_{10}H_8NO_2Cl$) were used to label fibroblasts and osteosarcoma, respectively. First, stock solutions were created for each cell type using dimethylsulfoxide for the CMAC solution and phosphate-buffered saline for the CM-DIL solution. The CM-DIL solution was diluted to a 2 μM concentration and the CMAC was diluted to a 25 μM concentration. Each was incubated for 15–45 min. Frozen cells were removed from the freezer and thawed in a water bath at 37°C. They were then centrifuged at 2000 r/min for 4 min to separate the cells from the supernatant. Osteosarcoma cells were then added to the CMAC solution and incubated for 30 min at 37°C while fibroblast cells were added to the CM-DIL solution and incubated for 5 min. The CM-DIL-fibroblast solution was then chilled for 15 min at 5°C. Each solution was then centrifuged at 2000 r/min for 4 min to remove the supernatant. This resulted in dying the fibroblast cells red with an excitement wavelength of 553 nm and emission wavelength of 570 nm, and dying the osteosarcoma cells blue with an excitement wavelength of 353 nm and emission wavelength of 466 nm. To estimate the initial cell viability after the staining, 100 μL of each solution was mixed with 100 μL of Trypan Blue and examined with a hemocytometer. The cell concentration was adjusted to approximately 100,000 cells/mL. Two-hundred microliters of osteosarcomas and fibroblasts were seeded to the random region and aligned region, respectively. The scaffolds were then incubated in complete growth medium (Eagle's minimal essential medium with 10% fetal bovine serum) at 37°C and monitored periodically for cellular growth.

Results

Scaffolds characterization

The SEM images of representative electrospun samples were shown in Figure 2. The anisotropic scaffolds are comprised of three regions: aligned fibers, random fibers, and the interface. The three regions are morphologically distinct but structurally continuous, and thus closely mimic the variation in collagen fiber orientation at the tendon/ligament-to-bone insertion site. The distribution of fiber orientation from a representative sample (15% PCL, 10-min duration, 20.5 cm height) was shown in Figure 3(a). The standard deviation of the orientation was considered when determining the overall alignment of each region. A summary of fiber alignment at the aligned sections for all eight groups was shown in Figure 3(b), where small degrees of orientation indicate a higher alignment (a perfect orientation, i.e. if all fibers are strictly aligned, will have a standard deviation of 1°). No statistical significance was found among the groups. Changing the process parameters

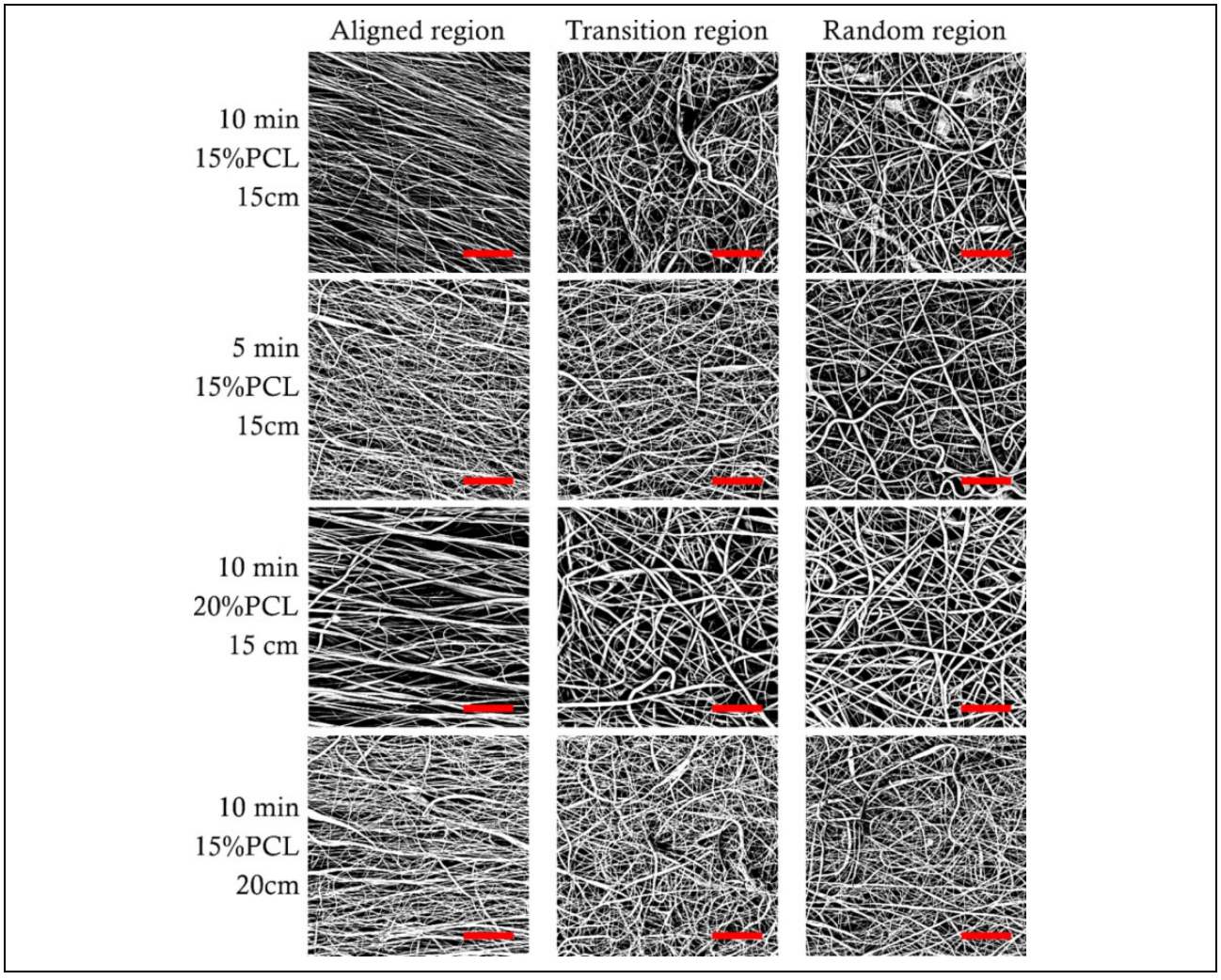

Figure 2. Electrospun sample pictures taken by the SEM. For each sample, a picture in the aligned, transition, and random regions was taken with a magnification of $\times 2000$ (scale bar $= 30$ μm). From the first row, each of the following samples was selected to have a direct comparison between each parameter (time, PCL concentration, distance). PCL: polycaprolactone. SEM: scanning electron microscopy.

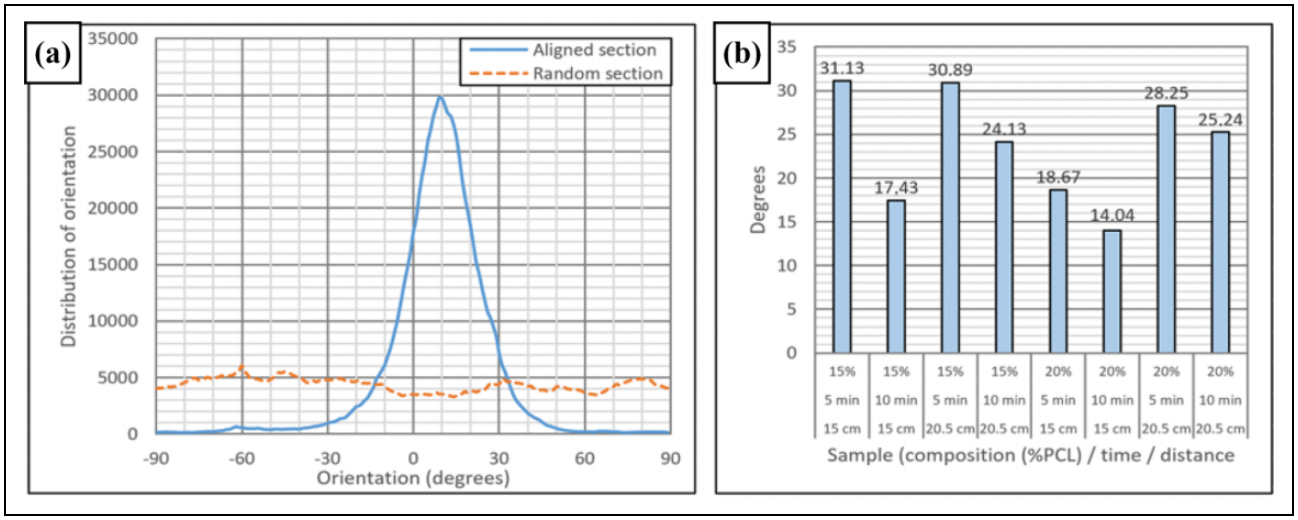

Figure 3. Results from the orientation analysis: (a) a sample fiber alignment plot (15% PCL, 10-min duration, 20.5 cm height) and (b) fiber alignment summary for the aligned regions of the scaffolds. PCL: polycaprolactone.

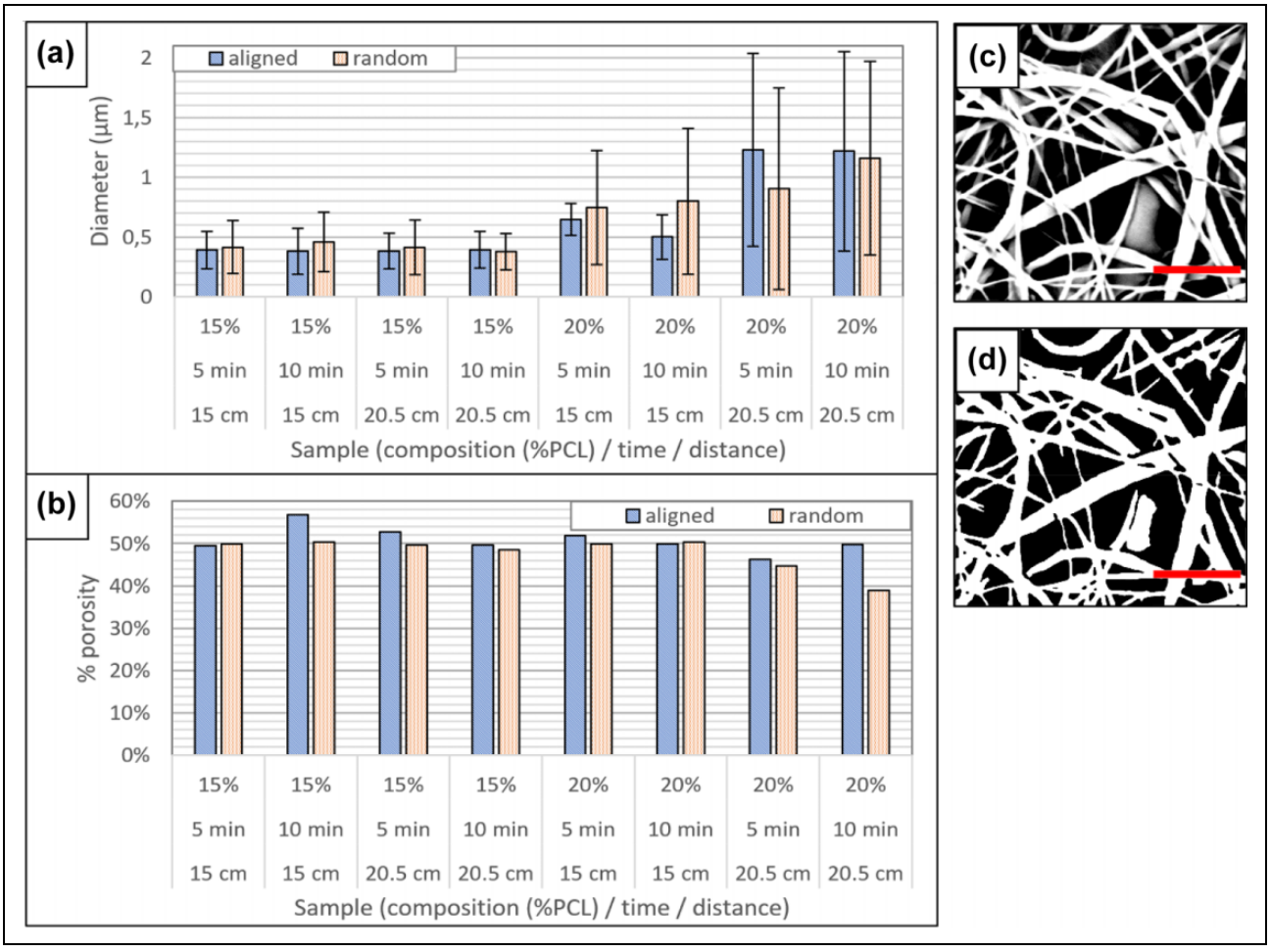

Figure 4. Results from the diameter and porosity analysis: (a) shows the diameter measured of each sample for the aligned and random region; (b) shows the porosity of each sample, calculated as the number of black pixels over the total number of pixels in the image; and (c) and (d) are images from the random region of the second sample (15% PCL, 10-min duration, 15 cm height) before and after the segmentation, respectively. Scale bar = 8 μm. PCL: polycaprolactone.

did not influence the nanofiber alignment at the aligned region of the scaffold.

The analysis consists of segmenting the picture to obtain a black-and-white image, as shown in Figure 4(c) and (d). Segmentation takes the grayscale images obtained from the SEM, as seen in Figure 4(c), and sets anything above a certain threshold of brightness to white, and everything else to black, as seen in Figure 4(d), which gives the images cutoffs for the software to calculate from. After that, the plug-in analyzed the picture and gave percent porosity and diameter of the fibers with the average and standard deviation. The PCL percentage was positively correlated to the nanofiber diameter mean as well as the standard deviation. Fifteen percent PCL solution resulted in smaller nanofibers with a higher consistency, while 20% PCL solution resulted in a wider distribution in fiber diameter. However, there was no substantial difference with regard to the overall porosity of the nanofiber scaffolds. Highly porous scaffolds were obtained in all eight groups.

Cellular growth

After 1 day of cellular growth, both cell types have adhered to the scaffolding for their respective regions. Red-dyed fibroblast cells had aligned with the aligned fibers, as seen in Figure 5. Blue-dyed osteosarcoma cells on the random region did not have any clear orientation. After 4 days, there is a noticeable increase in cell density for both regions. The fibroblasts in the aligned region have continued to grow aligned with the fibers of the scaffold. As expected, the osteosarcoma cells did not display any orientation on the random region.

The transition region, seen in Figure 6, had a mix of both fibroblast and osteosarcoma cells. Since this region was not directly seeded with cells, this indicates cellular migration to the transition region. There did not appear to be fibroblast migration to the random region or osteosarcoma migration to the aligned region by day 4. There cells also did not appear to display any pattern of alignment along the transition region.

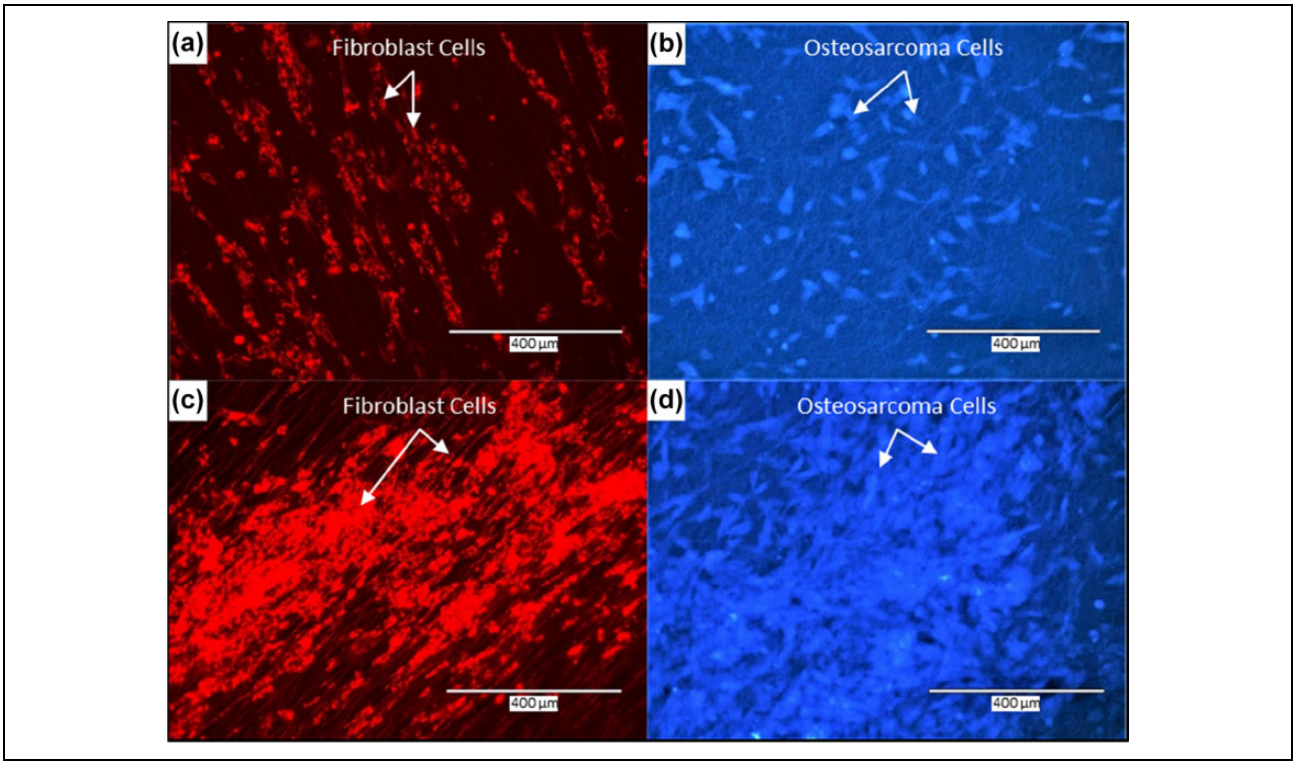

Figure 5. (a) Day 1 results for aligned region; (b) day 1 results for random region; (c) day 4 results for aligned region; and (d) day 4 results for random region. Fibroblast cells were dyed red and osteosarcoma cells were dyed blue.

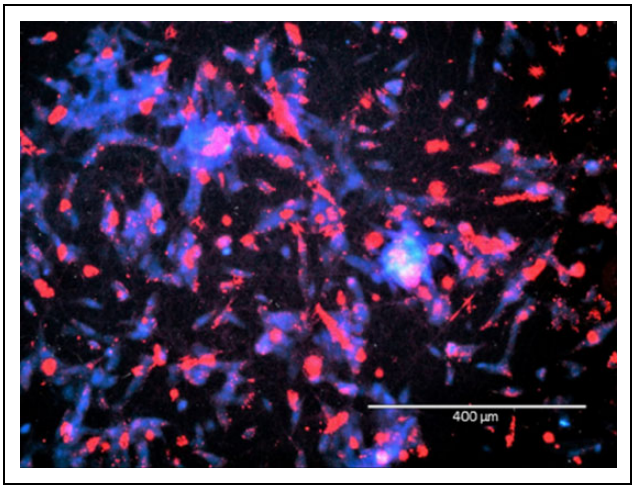

Figure 6. Example of scaffold transition region 4 days after cellular seeding.

Discussion

The electrospinning process used produces a relatively thin mat, which is usable for experimentation but is not representative of the full three-dimensional (3D) structure of a natural tendon and tendon-to-bone interface. Stacking multiple spun mats on top of each other creates a structure more akin to natural tissue.[17] Cellular seeding can be done on a layer by layer basis as well, giving better control over the cell growth.[17] Xie et al. first introduced an electrospinning configuration to fabricate an "aligned-to-random" fibrous scaffold by adopting a collector composed of two stapler-shaped metal frames.[1] Fibroblasts cultured on this scaffold exhibited a morphology gradient induced by the fiber organization. Li et al. designed a continuously graded, bone-like calcium phosphate coating on a nonwoven mat of electrospun fibers.[18] The gradient in mineral content resulted in a gradient in the stiffness of the scaffold and further influenced the activity of mouse pre-osteoblast MC3T3 cells. Rothrauff et al. compared two designs, stacked or braided, of multilayered scaffolds of aligned electrospun fibers.[19] Human bone marrow-derived mesenchymal stem cells were seeded on both types of scaffolds. It was found that braided scaffolds exhibited improved tensile and suture retention strengths, but cell infiltration was superior in stacked constructs, resulting in enhanced cell number, total collagen content, and total sulfated glycosaminoglycan content.

In our study, we integrated the ECM microstructure gradient and cellular heterogeneity for enthesis regeneration. Natural entheses exhibit gradients in tissue organization, composition, and mechanical properties that serve to effectively transfer stress between mechanically dissimilar materials and sustain the heterotypic cellular communications required for interface function and homeostasis.[20] The aligned and parallel collagen fibers at the tendon/ligament start bending and intercrossing along the insertion, change their orientation, and become more disorganized closer to

the bone.[6] Through the parallel electrospinning technique, we fabricated biomimic nanofiber scaffolds for the enthesis. The aligned region, random region, and interface region were morphologically distinct but structurally continuous, which closely mimicked the variation in collagen fiber orientation at the tendon/ligament-to-bone insertion site. The pore size and porosity of the scaffold were determined by the microfiber diameter and density.

While PCL was chosen as the single material in the experiment, multiple materials with different mechanical properties, more similar to the tissue in the interface, could be used for scaffold creation.[14] The scaffold surface could be modified in its entirety or selectively after spinning to increase cell adhesion and growth.[6] Co-electrospinning, or the spinning of multiple materials at once, can be done using multiple needles or using a single coaxial needle to create fibers with one material coated by another.[9] It is possible to incorporate nanoparticles into the electrospun solution, and subsequently grow material off those nanoparticles to better recreate bone.[21] The combination of some of these techniques with a multi-region scaffold as created in this experiment could greatly improve the mechanical and biological characteristics of the electrospun scaffold in future experimentation.

Overall, the alignment of our samples in the aligned regions was in agreement with other studies, where it is estimated that an azimuthal orientation of 20° is very high for this PCL percentage.[22] We observed that the fiber alignment for the aligned section was better in the 10-min samples than the 5-min samples. This may have occurred due to fiber deposition between the parallel bars being inconsistent in the alignment during the first few minutes of electrospinning, and the 5-min samples were not thick enough to fully cover these initial fiber layers. Twenty percent PCL solution had better alignment than 15%, however, further analysis is needed to confirm this. The sample which showed the best alignment was produced with 20% PCL solution at a height of 15 cm for 10 min.

Average fiber diameter and sample porosity analysis results are presented in Figure 3. For each set of parameters, the diameter did not significantly change between the random and aligned regions. These results are in accordance with what can been seen in terms of diameters[23–25] and porosity.[26] With DMF as solvent, similar fiber diameters were observed (between 300 nm and 2 μm). The PCL concentration played an influential role when determining the average fiber diameter. Fifteen percent PCL sample diameters were around 0.39 μm whereas 0.8 μm mean value was observed for 20% PCL samples, which complies with other studies.[27] However, the normal variation between mean diameters should have been around 60%. While 15% PCL samples agree with this data, large variations were observed in 20% PCL samples (around 70% to 90%). The higher viscosity of the 20% PCL solution, coupled with the voltage being similar for all samples, may explain the variations for the 20% PCL samples, particularly for the 20.5 cm sample. While the voltage may have been enough to keep the diameter consistent for the lower viscosity 15% PCL solution, the electric field generated during electrospinning may not have had the strength to spin the 20% PCL solution to the same diameter, and the weaker field resulting from the larger distance may have exacerbated the problem. Further testing with greater variations in voltages may be necessary to test for this. The inconsistency between each electrospun sample might have also played a role in these abnormal variations. A change in the solvent might be needed to better control the fiber diameter.[23] Since fiber diameter has been shown to affect fibroblast cells, precise control over fiber diameter would improve cell growth characteristics.[28]

Fiber porosity remained consistent between samples at approximately 50%. There were slight increases in porosity in the aligned section when compared to the corresponding random section, but not substantial. The material was then porous enough to accept cells and allow for proliferation.[29] After examining the cell culture results, there are a few noticeable outcomes worth mentioning. The increase in cell density along with the configuration of the fibroblast cells along the aligned region (Figure 3) shows promising biocompatibility for the electrospun scaffold. Similarly, the scaffold shows cell migration across both regions into the transition region (Figure 4). Previous studies using fibroblasts on electrospun scaffolds have shown similar results with cell proliferation and alignment along the aligned region of the scaffold, as well as cell migration abilities.[30] The effect of electrospun PCL scaffold alignment on Schwann cell maturation was also reported, and results showed that cells cultured on the aligned region aligned and elongated along the fiber axes, which they attribute to a phenomenon known as contact guidance.[31] This form of cellular alignment is also commonly seen among other studies using human fibroblasts and Schwann cells.[32,33] Additionally, a recent study was conducted in which natural polymers were used to create nanoparticles for electrospinning, which was found to create scaffolds with improved cell viability and attachment.[34] Additional experimentation may be required to compare other solutions to PCL to potentially improve cell interaction. If a clinically usable product is to mimic the cell characteristics of the bone–tendon interface, it must have high levels of biocompatibility along with cell migration capabilities, which our scaffold appears to demonstrate.

To help determine if the observed cellular activity represents an effective interaction between the cells and their environment, previous studies have often focused on a few key factors. First, the biological functionality of the cells can be generally determined based on whether they are able to maintain normal phenotypic shape within the scaffold.[35] Second, cell adherence to the scaffold along with proliferation within the nanofibrous network suggests cell approval of the structure.[35] Finally, researchers often examine the cross-sectional cellular activity to determine if the cells

integrate with multiple layers of the scaffold to form a 3-D network.[35,36] In this study, microtopographical cues, coupled with the intercellular interactions promoted the enthesis formation. While our cell culture analysis demonstrates the first two factors, a follow-up study could be conducted to examine the 3-D capabilities of osteoblasts, fibroblasts, and chondrocytes on a single gradient scaffold.

It is reported that in the United States, about 250,000 anterior cruciate ligament injuries occur annually,[37] and between 200,000 and 300,000 rotator cuffs are surgically repaired each year.[38] This study provides a multicellular strategy to engineer tendon/ligament-to-bone interface (enthesis). It will not only promote future development of regenerative medicine enabling functional and integrative recovery of tendon/ligament-to-bone injuries, but may also inspire new strategies toward organ-on-chip for heterogeneous tissues. Future work includes incorporating nanoparticles and growth factors to create a multifunctional microenvironment for improvement of cellular growth as well as mechanical properties of the engineered tissues.

Conclusion

This article presents a novel technique for tendon–bone tissue regeneration. We adopted a parallel electrospinning method to fabricate the random-to-aligned nanofiber scaffolds. Fibroblasts and osteosarcoma cells were seeded on designated areas and cocultured in the scaffold. The microtopology, specifically the nanofiber alignment, guided the cell organization. The cocultured construct mimicked the tendon–bone interface microstructure. This article provides an effective biomimetic model for tendon/ligament regeneration, and can be further developed as an organ-on-chip or a therapeutic alternative for heterogeneous tissues.

Declaration of Conflicting Interests

The author(s) declared no potential conflicts of interest with respect to the research, authorship, and/or publication of this article.

Funding

The author(s) disclosed receipt of the following financial support for the research, authorship, and/or publication of this article: This work was financially supported by the Texas Tech University Startup Initiative.

References

1. Xie J, Li X, Lipner J, et al. "Aligned-to-random" nanofiber scaffolds for mimicking the structure of the tendon-to-bone insertion site. *Nanoscale* 2010; 2: 923–926.
2. Lu HH, Subramony SD, Boushell MK, et al. Tissue engineering strategies for the regeneration of orthopedic interfaces. *Annal Biomed Eng* 2010; 38: 2142–2154.
3. Thomopoulos S, Williams GR, Gimbel JA, et al. Variation of biomechanical, structural, and compositional properties along the tendon to bone insertion site. *J Orthop Res* 2003; 21: 413–419.
4. Sharma P and Maffulli N. Biology of tendon injury: healing, modeling and remodeling. *J Musculos Neuron Interact* 2006; 6: 181–190.
5. Linderman SW, Golman M, Gardner TR, et al. Enhanced tendon-to-bone repair through adhesive films. *Acta Biomater* 2018; 70: 165–176.
6. Font Tellado S, Balmayor ER, and Van Griensven M. Strategies to engineer tendon/ligament-to-bone interface: biomaterials, cells and growth factors. *Adv Drug Delivery Rev* 2015; 94: 126–140.
7. Vacanti JP and Langer R. Tissue engineering: the design and fabrication of living replacement devices for surgical reconstruction and transplantation. *Lancet (London, England)* 1999; 354(Suppl 1): Si32–Si34.
8. Moffat KL, Kwei AS, Spalazzi JP, et al. Novel nanofiber-based scaffold for rotator cuff repair and augmentation. *Tissue Eng A* 2009; 15: 115–126.
9. Sahay R, Thavasi V, and Ramakrishna S. Design modifications in electrospinning setup for advanced applications. *J Nanomater* 2011; 2011: 7.
10. Shin SH, Purevdorj O, Castano O, et al. A short review: recent advances in electrospinning for bone tissue regeneration. *J Tissue Eng* 2012; 3: 2041731412443530.
11. Doustgani A and Ahmadi E. Melt electrospinning process optimization of polylactic acid nanofibers. *J Ind Text* 2016; 45: 626–634.
12. Pant HR, Neupane MP, Pant B, et al. Fabrication of highly porous poly (varepsilon-caprolactone) fibers for novel tissue scaffold via water-bath electrospinning. *Colloids Surf B Biointerfaces* 2011; 88: 587–592.
13. Drexler JW and Powell HM. Regulation of electrospun scaffold stiffness via coaxial core diameter. *Acta Biomater* 2011; 7: 1133–1139.
14. Ladd MR, Lee SJ, Stitzel JD, et al. Co-electrospun dual scaffolding system with potential for muscle–tendon junction tissue engineering. *Biomaterials* 2011; 32: 1549–1559.
15. Samavedi S, Olsen Horton C, Guelcher SA, et al. Fabrication of a model continuously graded co-electrospun mesh for regeneration of the ligament–bone interface. *Acta Biomater* 2011; 7: 4131–4138.
16. Du L, Xu H, Zhang Y, et al. Electrospinning of polycaprolatone nanofibers with DMF additive: the effect of solution proprieties on jet perturbation and fiber morphologies. *Fiber Polym* 2016; 17: 751–759.
17. Sankar S, Sharma CS, Rath SN, et al. Electrospun fibers for recruitment and differentiation of stem cells in regenerative medicine. *Biotechnol J* 2017; 12: 1700263.
18. Li X, Xie J, Lipner J, et al. Nanofiber scaffolds with gradations in mineral content for mimicking the tendon-to-bone insertion site. *Nano Lett* 2009; 9: 2763–2768.
19. Rothrauff BB, Lauro BB, Yang G, et al. Braided and stacked electrospun nanofibrous scaffolds for tendon and ligament tissue engineering. *Tissue Eng A* 2017; 23: 378–389.
20. Lu HH and Thomopoulos S. Functional attachment of soft tissues to bone: development, healing, and tissue engineering. *Annual Rev Biomed Eng* 2013; 15: 201–226.

21. Li X, Cheng R, Sun Z, et al. Flexible bipolar nanofibrous membranes for improving gradient microstructure in tendon-to-bone healing. *Acta Biomater* 2017; 61: 204–216.
22. Liu J, Lin DY, Wei B, et al. Single electrospun PLLA and PCL polymer nanofibers: increased molecular orientation with decreased fiber diameter. *Polymer (Guildf)* 2017; 118: 143–149.
23. Katsogiannis KAG, Vladisavljević GT, and Georgiadou S. Porous electrospun polycaprolactone (PCL) fibres by phase separation. *Eur Polym J* 2015; 69: 284–295.
24. Liverani L and Boccaccini AR. Versatile production of poly (epsilon-caprolactone) fibers by electrospinning using benign solvents. *Nanomaterials* 2016; 6: 75.
25. Gholipour Kanani A and Bahrami SH. Effect of changing solvents on poly(ϵ-caprolactone) nanofibrous webs morphology. *J Nanomater* 2011; 2011: 1–10.
26. Blakeney BA, Tambralli A, Anderson JM, et al. Cell infiltration and growth in a low density, uncompressed three-dimensional electrospun nanofibrous scaffold. *Biomaterials* 2011; 32: 1583–1590.
27. Pisani S, Dorati R, Conti B, et al. Design of copolymer PLA-PCL electrospun matrix for biomedical applications. *React Funct Polym* 2018; 124: 77–89.
28. Erisken C, Zhang X, Moffat KL, et al. Scaffold fiber diameter regulates human tendon fibroblast growth and differentiation. *Tissue Eng A* 2013; 19: 519–528.
29. Hollister SJ. Porous scaffold design for tissue engineering. *Nature Mater* 2005; 4: 518–524.
30. Mi HY, Salick MR, Jing X, et al. Electrospinning of unidirectionally and orthogonally aligned thermoplastic polyurethane nanofibers: fiber orientation and cell migration. *J Biomed Mater Res A* 2015; 103: 593–603.
31. Chew SY, Mi R, Hoke A, et al. The effect of the alignment of electrospun fibrous scaffolds on Schwann cell maturation. *Biomaterials* 2008; 29: 653–661.
32. Lee CH, Shin HJ, Cho IH, et al. Nanofiber alignment and direction of mechanical strain affect the ECM production of human ACL fibroblast. *Biomaterials* 2005; 26: 1261–1270.
33. Schnell E, Klinkhammer K, Balzer S, et al. Guidance of glial cell migration and axonal growth on electrospun nanofibers of poly-epsilon-caprolactone and a collagen/poly-epsilon-caprolactone blend. *Biomaterials* 2007; 28: 3012–3025.
34. Sheikh FA, Ju HW, Moon BM, et al. A comparative mechanical and biocompatibility study of poly(ϵ-caprolactone), hybrid poly(ϵ-caprolactone)–silk, and silk nanofibers by colloidal electrospinning technique for tissue engineering. *J Bioact Compatible Polym* 2014; 29: 500–514.
35. Li WJ, Laurencin CT, Caterson EJ, et al. Electrospun nanofibrous structure: a novel scaffold for tissue engineering. *J Biomed Mater Res* 2002; 60: 613–621.
36. Matthews JA, Wnek GE, Simpson DG, et al. Electrospinning of collagen nanofibers. *Biomacromolecules* 2002; 3: 232–238.
37. Grindem H, Snyder-Mackler L, Moksnes H, et al. Simple decision rules can reduce reinjury risk by 84% after ACL reconstruction: the Delaware-Oslo ACL cohort study. *Br J Sports Med* 2016; 50: 804–808.
38. Colvin AC, Egorova N, Harrison AK, et al. National trends in rotator cuff repair. *J Bone Joint Surg Am Vol* 2012; 94: 227.